

Overactivity or blockade of transforming growth factor- β each generate a specific ureter malformation

Filipa M Lopes¹, Neil A Roberts¹, Leo AH Zeef², Natalie J Gardiner³ and Adrian S Woolf^{1,4*} 

¹ Division of Cell Matrix Biology and Regenerative Medicine, School of Biological Sciences, Faculty of Biology Medicine and Health, University of Manchester, Manchester, UK

² The Bioinformatics Core Facility, University of Manchester, Manchester, UK

³ Division of Diabetes, Endocrinology and Gastroenterology, School of Medical Sciences, Faculty of Biology, Medicine and Health, University of Manchester, Manchester, UK

⁴ Royal Manchester Children's Hospital, Manchester University NHS Foundation Trust, Manchester Academic Health Science Centre, Manchester, UK

*Correspondence to: AS Woolf, Division of Cell Matrix Biology and Regenerative Medicine, School of Biological Sciences, Faculty of Biology Medicine and Health, University of Manchester, Michael Smith Building, Oxford Road, Manchester M13 9PT, UK. E-mail: adrian.woolf@manchester.ac.uk

Abstract

Transforming growth factor- β (TGF β) has been reported to be dysregulated in malformed ureters. There exists, however, little information on whether altered TGF β levels actually perturb ureter development. We therefore hypothesised that TGF β has functional effects on ureter morphogenesis. *Tgfb1*, *Tgfb2* and *Tgfb3* transcripts coding for TGF β ligands, as well as *Tgfr1* and *Tgfr2* coding for TGF β receptors, were detected by quantitative polymerase chain reaction in embryonic mouse ureters collected over a wide range of stages. As assessed by *in situ* hybridisation and immunohistochemistry, the two receptors were detected in embryonic urothelia. Next, TGF β 1 was added to serum-free cultures of embryonic day 15 mouse ureters. These organs contain immature smooth muscle and urothelial layers and their *in vivo* potential to grow and acquire peristaltic function can be replicated in serum-free organ culture. Such organs therefore constitute a suitable developmental stage with which to define roles of factors that affect ureter growth and functional differentiation. Exogenous TGF β 1 inhibited growth of the ureter tube and generated cocoon-like dysmorphogenesis. RNA sequencing suggested that altered levels of transcripts encoding certain fibroblast growth factors (FGFs) followed exposure to TGF β . In serum-free organ culture exogenous FGF10 but not FGF18 abrogated certain dysmorphic effects mediated by exogenous TGF β 1. To assess whether an endogenous TGF β axis functions in developing ureters, embryonic day 15 explants were exposed to TGF β receptor chemical blockade; growth of the ureter was enhanced, and aberrant bud-like structures arose from the urothelial tube. The muscle layer was attenuated around these buds, and peristalsis was compromised. To determine whether TGF β effects were limited to one stage, explants of mouse embryonic day 13 ureters, more primitive organs, were exposed to exogenous TGF β 1, again generating cocoon-like structures, and to TGF β receptor blockade, again generating ectopic buds. As for the mouse studies, immunostaining of normal embryonic human ureters detected TGF β RI and TGF β RII in urothelia. Collectively, these observations reveal unsuspected regulatory roles for endogenous TGF β in embryonic ureters, fine-tuning morphogenesis and functional differentiation. Our results also support the hypothesis that the TGF β up-regulation reported in ureter malformations impacts on pathobiology. Further experiments are needed to unravel the intracellular signalling mechanisms involved in these dysmorphic responses.

© 2019 The Authors. *The Journal of Pathology* published by John Wiley & Sons Ltd on behalf of Pathological Society of Great Britain and Ireland.

Keywords: embryo; growth factor; human; malformation; mouse; urothelium

Received 31 October 2018; Revised 19 July 2019; Accepted 6 August 2019

No conflicts of interest were declared.

Introduction

The mammalian ureter connects the kidney with the bladder. Cadherin-1 (CDH1) is located at urothelial intercellular junctions and in the mature organ uroplakin (UPK) proteins coat the luminal surface of

the pseudostratified urothelium, conferring waterproofing properties [1]. The urothelium is surrounded by smooth muscle (SM) cells expressing contractile proteins including α -SM actin (α SMA) and the intermediate filament desmin [2,3]. The SM is surrounded by adventitial fibrocytes. Between the urothelium and SM lie the

lamina propria interstitial cells. The ureter propels urine in a proximal (i.e. near the kidney) to distal direction [3]. Contractions are initiated by pacemaker cells near the renal pelvis [4], and peristaltic waves are propagated by Cajal-like cells [5].

The ureter epithelium originates when the ureteric bud branches from the mesonephric duct [6]. The bud elongates and its stalk differentiates into urothelia. Mesenchymal cells condense around the urothelial stalk, differentiating into SM [7]. The distal end of the stalk joins the bladder [8]. In mice, the bud initiates at embryonic day 10 (E10). The bud elongates and becomes surrounded by condensed mesenchyme. At E13 the latter compartment has differentiated so that the inner cells begin to express SM molecules and the outer cells form adventitia [2]. At E15 the primitive urothelium has differentiated into basal and superficial cell layers [2]. Over the next few prenatal days the ureter begins to transmit urine generated by the metanephros [7], with the urothelium having three cell layers by E18 [2]. In humans, the bud initiates at 5 weeks gestation and the 10-week ureter contains a multi-layered urothelium surrounded by SM [9].

Human ureter malformations can be visualised upon foetal ultrasonographic screening [10]. Mild dilation is detected in 5% of foetuses [11]. Most are transient anomalies whereas in other individuals dysmorphic ureters persist postnatally [11]. Some of these are secondary to primary diseases that prevent urine flow, such as bladder outflow obstruction [12]. Other malformations represent intrinsic defects of ureter morphogenesis, ranging from an absent organ to a ureter which has either an occluded lumen or a patent lumen but with dysfunctional peristalsis. Ureter malformations can co-exist with dysplastic kidneys containing poorly differentiated and metaplastic cells [12].

Molecules in the transforming growth factor- β (TGF β) axis have been detected in both kidney and ureter malformations. In human dysplastic kidneys TGF β 1 immunostaining is prominent in metaplastic SM enveloping dysplastic tubules that themselves express TGF β RI and TGF β RII [13], cell surface receptors activated by TGF β 1–3 ligands [14]. Exposing cultured human dysplastic kidney epithelia to TGF β 1 leads to up-regulated fibronectin [13]. In organ culture of mouse metanephric kidneys, exogenous TGF β 1 inhibits tubule formation, whereas blocking endogenous TGF β 1 enhances tubulogenesis [15]. Experimental urinary flow obstruction in foetal sheep generates dysmorphic kidney tubules, with increased TGF β 1, TGF β RI and TGF β RII [16]. TGF β 1 has been detected in congenital stenotic ureters and megaureters [17–19] and ureteric ligation in postnatal rats up-regulated TGF β 1 and its receptors in the ureter capsule [20].

Given that TGF β pathway molecules have been reported to be up-regulated in both human kidney and ureter malformations, we here first examined normal human embryos, immunodetecting both TGF β RI and TGF β RII in developing ureters. Key components of the TGF β axis were detected in embryonic mouse ureters

using RT-qPCR, *in situ* hybridisation and immunohistochemistry. Hypothesising that TGF β mediates ureter morphogenesis, we added TGF β 1 to serum-free organ cultures of mouse E15 ureters. These organs contain immature SM and urothelial layers and their *in vivo* potential to grow and acquire peristaltic function can be replicated in serum-free organ culture, as demonstrated previously [3] and in this study. E15 ureters thus constitute a suitable stage of development with which to define roles of factors that may perturb or enhance ureter growth and functional differentiation. Exogenous TGF β 1 inhibited growth of the ureter tube and generated cocoon-like dysmorphogenesis. RNA-sequencing suggested TGF β altered levels of numerous transcripts, including *Fgf18* and *Fgf10* that code for fibroblast growth factors (FGFs). Given that little is known about the roles of these molecules in ureter development, we added them to serum-free embryonic ureter cultures. FGF10 but not FGF18 abrogated certain dysmorphic effects mediated by exogenous TGF β 1. To assess whether an endogenous TGF β axis operates in developing ureters, E15 explants were exposed to TGF β receptor blockers. Here, aberrant bud-like structures arose from the urothelial tube and the rate of peristalsis was decreased.

Materials and methods

Ethics

Human tissues, collected after maternal consent and ethical approval (REC 08/H0906/21+5), were provided by the MRC and Wellcome Trust Human Developmental Biology Resource (<http://www.hdbr.org/>). CD1 wild-type strain mouse experiments were approved by the University of Manchester ethics committee and UK Home Office (licence PAFFCI44F).

Organ culture

Embryonic ureters were explanted onto platforms (0.4 μ m; Millipore, Watford, UK) and cultured for 6 days [3,21]. Explants were fed DMEM/F12 (D8437, Sigma-Aldrich, Gillingham, UK) containing insulin–transferrin–selenium (41400045, Gibco, Life Technologies, Paisley, UK) and penicillin–streptomycin (Thermo Fisher Scientific, Paisley, UK). Media were renewed at day 3. In some experiments the following were added: recombinant human TGF β 1 (240-B; R&D Systems, Minneapolis, MN, USA); TGF β R inhibitor LY2109761 (A8464, Generon, Slough, UK); TGF β R inhibitor SB431542 (04-0010; Generon); recombinant mouse FGF18 (CYT-064; ProSpec, Ness-Ziona, Israel); recombinant mouse FGF10 (6224-FG-025, R&D Systems); and 5-bromo-2'-deoxyuridine (BrdU; B5002-100MG, Sigma-Aldrich), applied 2 h before harvest. Photographs were taken using inverted light microscope (Leica M80; Leica Microsystems, Milton Keynes, UK). Growth was assessed using ImageJ

software (National Institutes of Health, Bethesda, MD, USA). For linear growth, a line drawn down the middle of the ureter tube was measured. To measure ureter tube area, a line was drawn around the epithelium plus SM layer. These two parameters give a more sophisticated view of growth than that based on just one dimension. On day 6, the number of waves of peristalsis initiating in the proximal ureter during 2 min was counted by direct inspection using an Eclipse Ti inverted microscope (Nikon UK, Kingston upon Thames, UK) maintaining explants at 37 °C in 5% CO₂ [21]. Statistical comparisons were made using Student's *t*-test, Mann–Whitney or Kruskal–Wallis tests, as appropriate, adjusting for multiple comparisons when appropriate.

RNA sequencing

RNA-sequencing was undertaken, as described previously [22–25] and detailed in supplementary material, Supplementary materials and methods. Data was deposited in the ArrayExpress repository (E-MTAB-7395).

Histology, RT-qPCR and *in situ* hybridisation

Please see supplementary material, Supplementary materials and methods for details.

Results

Human ureters

Ureters in a 7-week gestation embryo contained epithelial tubes, with walls one to two cells thick, that were immunopositive for CDH1 but not for UPKII, surrounded by mesenchyme-like cells with α SMA immunostaining barely detectable (Figure 1). Ureters of a 10-week gestation embryo had urothelium, with multiple layers, immunopositive for CDH1. UPKII immunostaining was detected on the luminal aspect of the urothelial layer, and cells around the urothelium immunostained for α SMA. Picrosirius red, a collagen-reactive dye [26], stained a basement membrane-like line around urothelia at 7 weeks, a signal more prominent at 10 weeks. At both ages, epithelia immunostained for TGF β RI and TGF β RII. pSMAD2, a TGF β canonical intracellular signalling molecule [14] was detected in subsets of epithelia and surrounding cells. Fluorescence immunohistochemistry was undertaken in a separate late first trimester specimen, detecting a plasma membrane-like localisation of TGF β RI and TGF β RII in urothelia (see supplementary material, Figure S1).

Mouse ureters *in vivo*

The E15 mouse ureter (Figure 2) consisted of an epithelial tubule, two cells deep, immunostaining for CDH1 but not UPKII. The tube was surrounded by a nascent SM layer expressing α SMA. In the CD1 mice used here,

birth occurs at 21 days of gestation i.e. 6 days after E15. Neonates (Figure 2) had a multi-layered urothelium that was immunopositive for CDH1 and UKPII, surrounded by α SMA expressing SM. Picrosirius red staining revealed a basement membrane-like patterns on the abluminal border of the E15 epithelium while neonatally the most prominent signal was in the adventitia. Bright-field peroxidase-based immunohistochemistry (Figure 2) showed signals for TGF β RI and TGF β RII in E15 and neonatal ureters. Fluorescence immunohistochemistry at E15 detected a plasma membrane like pattern for TGF β RI and TGF β RII in the urothelium (see supplementary material, Figure S2). We undertook RT-qPCR for *Tgfb1*, *Tgfb2*, *Tgfb3*, *Tgfb1* and *Tgfb2* using mRNA from freshly dissected mouse ureters. These results (see supplementary material, Figure S3), showed that all were expressed over a wide span of mouse ureter development i.e. at embryonic days 13, 15 and 18, and on the day of birth. Given that a focus of our functional experiments were E15 explants, below, *in situ* hybridisation was undertaken for *Tgfb1*, *Tgfb1* and *Tgfb2* on E15 ureters (see supplementary material, Figure S4). Sparse signals for *Tgfb1* were detected. More prominent signals were detected for *Tgfb1* and *Tgfb2*. Both receptor mRNAs were detected in the epithelium, consistent with the immunohistochemical data for TGF β RI and TGF β RII, showing that this layer is equipped with two key receptors to bind and initiate signalling by TGF β ligands. *Tgfb2* was also detected in lamina propria, SM and adventitia.

TGF β axis molecules in embryonic ureter culture

As expected [3,21], E15 explants fed serum-free control media alone grew over 6 days, elongating an average of 1.2 mm, and increasing in area by an average of 0.3 mm² (see supplementary material, Figure S5). From 2 days, as expected [3,21], explants displayed spontaneous peristalsis. RNA-sequencing at one and 6 days confirmed epithelial molecular maturation, with increased levels of transcripts encoding UPKIa, UPKIb, UPKII and UPKIIIa (each *p* < 0.05, corrected for multiple comparisons). Transcripts encoding α SMA were expressed at both times with a non-significant increase, while transcripts for desmin, a SMC protein up-regulated later than α SMA *in vivo* in embryonic urinary tracts [27], showed a significant (*p* < 0.05) increase between days 1 and 6. We sought transcripts encoding TGF β axis members in the array (see supplementary material, Table S1). *Tgfb1*, *Tgfb2* and *Tgfb3* were robustly expressed (average reads >100) on days 1 and 6. *Tgfb1* significantly (*p* = 0.003, after adjusting for multiple comparisons) increased during culture, while *Tgfb2* and *Tgfb3* tended to fall. *Tgfb1* and *Tgfb2* were robustly expressed, as was *Tgfb3* encoding TGF β RIII, or betaglycan, a proteoglycan that sequesters TGF β [28].

Effects of exogenous TGF β 1

Basal media was supplemented with TGF β 1 at concentrations similar to those used when exploring effects

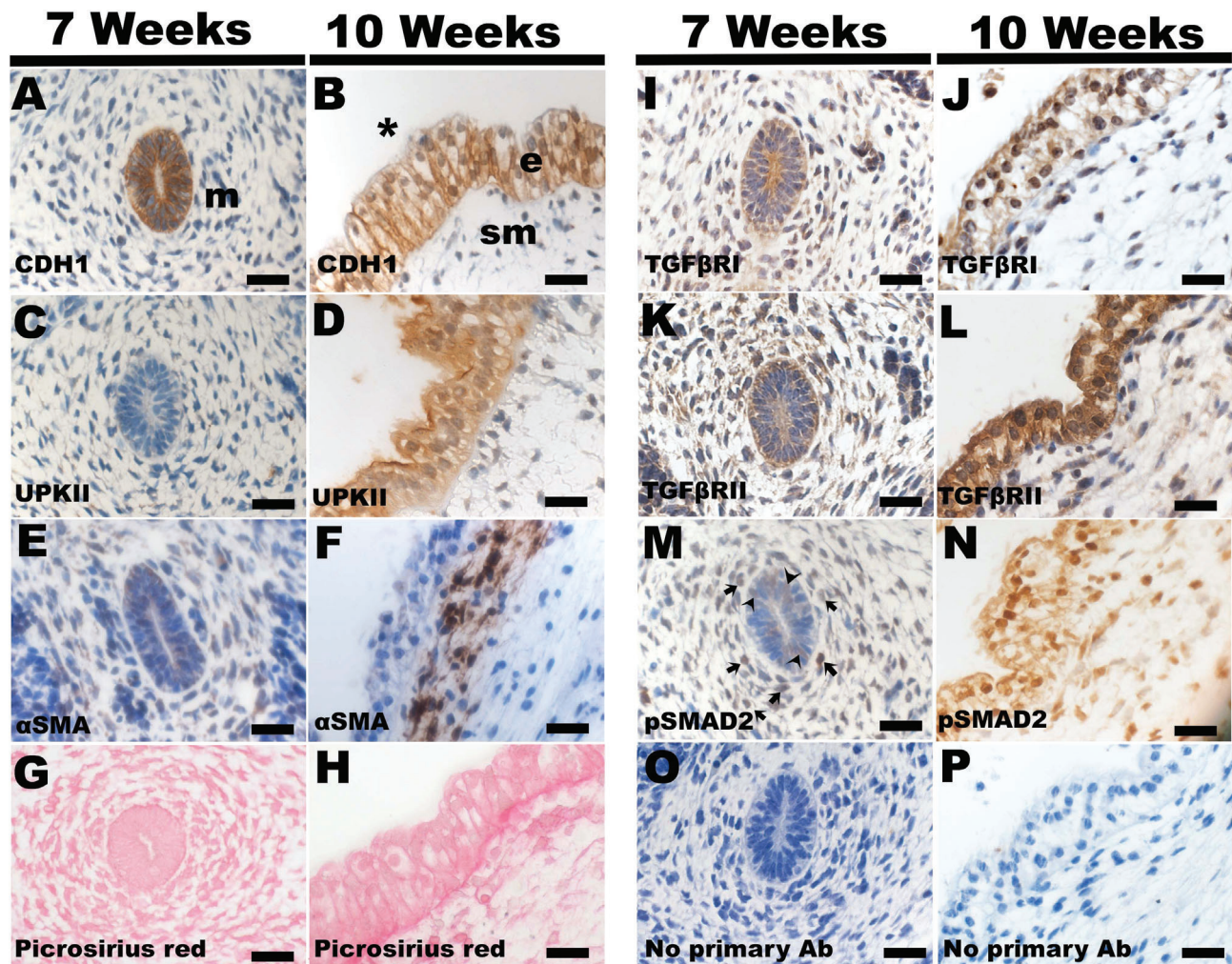


Figure 1. Histology of human embryonic ureters. (A,C,E,G,I,K,M,O) Transverse section of ureter from a 7-week embryo. (B,D,F,H,J,L,N,P) Longitudinal section of proximal ureter from a 10-week embryo. All sections were counterstained with haematoxylin (blue) apart from G and H. At 7 weeks CDH1 was detected (brown) in the primitive urothelium (A; *m* indicates mesenchyme), with expression maintained at 10 weeks in the multi-layered urothelium (B; *sm* indicates SM layer and the asterisk is in the lumen). At 7 weeks UPKII was not immunodetected (C) and α SMA was faintly detected in a subset of mesenchyme-like cells (D). Both UPKII and α SMA were prominent at 10 weeks (D,F). Picrosirius red staining showed a faint line around the base of the urothelium at 7 weeks, with a stronger signal in this location at 10 weeks (G,H). TGF β RI and TGF β RII were immunodetected in urothelium at seven (I, K) and 10 weeks (J,L). pSMAD2 was detected in subsets of urothelial cells (*arrowhead* in M) and in subsets of surrounding cells (*arrow* in M) at 7 weeks. pSMAD2 was detected in subsets of urothelial and surrounding cells at 10 weeks (N). No primary antibody negative controls (O,P). Bars, 10 μ m.

of this molecule on mouse embryonic kidney, small intestine and salivary gland explants [15,29–31]. About 5 and 50 ng/ml concentrations were each able to alter explant morphology, detailed below. One ng/ml had no overt effect and was not studied further (not shown). After 2 days, 5 ng/ml TGF β 1 exposed explants began to acquire a ‘cocoon’, with a prominent adventitia, a dysmorphic appearance that became more marked by day 6 (Figure 3). Five ng/ml TGF β 1 significantly reduced length and area growth, as assessed on the final day of culture (Figure 4) but these explants underwent peristalsis as normal (Figure 4). Fifty ng/ml TGF β 1 had more marked effects, with day 6 organs resembling circular discs (not shown): these underwent peristalsis, showing they were viable.

To determine whether exogenous TGF β 1 effects were restricted to E15 organs, we also studied E13 rudiments

that is less differentiated than E15 organs [2]. E13 explants exposed to 5 ng/ml TGF β 1 also acquired a cocoon-like phenotype (see supplementary material, Figure S6).

Hereafter, we mostly focused on E15 rudiments exposed to 5 ng/ml TGF β 1. The histology of dysmorphic explants harvested day 6 (Figure 5) showed prominent adventitia. The SM layer was intact and immunostained for α SMA, as in controls. The urothelium in both control explants and TGF β 1 exposed explants immunostained for CDH1 and UKPII. pSMAD2 immunostaining appeared prominent in TGF β 1 exposed cultures but was not quantified. We undertook proliferation assays with BrdU incorporation after 24 h of culture (see supplementary material, Figure S7), reasoning that any changes found would be less likely to reflect secondary effects from the

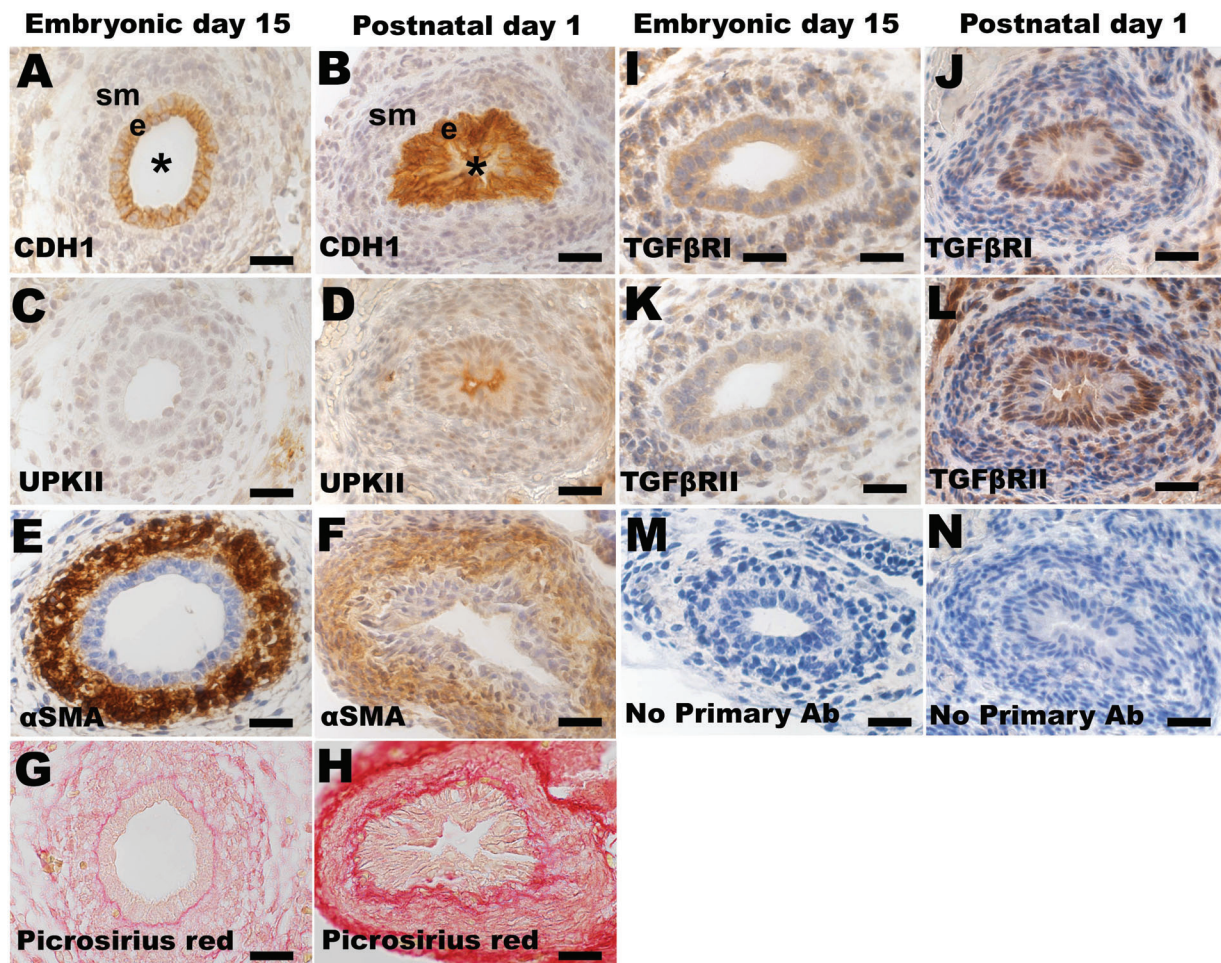


Figure 2. Histology and immunohistochemistry of mouse embryonic ureters. (A,C,E,G,I,K,M) Transverse sections of an E15 ureter within an intact embryo. (B,D,F,H,J,L,N) Transverse sections of ureter from a mouse on the day of birth. All sections were counterstained with haematoxylin (blue) apart from G and H. At E15 CDH1 was detected (brown) in the primitive urothelium (A); *e* indicates the epithelium, *sm* indicates the nascent SM layer, and the asterisk is in the lumen. At this age, UPKII was not detected in the epithelium (C), the surrounding cells expressed α SMA (E), and picrosirius red stained in a linear pattern adjacent to the base of the urothelium (G). In the neonatal ureter, both CDH1 (B) and UPKII (D) were detected in the urothelium, α SMA was detected in the SM layer (F), and picrosirius red staining was prominent in the putative interstitial layer adjacent to the urothelium, and in the adventitia (H). TGF β RI and TGF β RII were immunodetected in the E15 (I,K) and neonatal (J,L) ureter. No primary antibody negative controls (M,N). Bars, 20 μ m.

cocooning that became prominent later on. No significant differences were found between controls and TGF β 1-exposed organs in either epithelial, SM or adventitial layers.

FGFs in ureter cultures

We compared RNA-sequencing datasets in TGF β 1-exposed and control explants harvested after 24 h. After adjustment for multiple comparisons, levels of several hundred species of transcripts differed significantly. The most significantly changed transcripts are listed in supplementary material, Table S2, with the full set deposited in the ArrayExpress repository (E-MTAB-7395). Transcripts considered in the Discussion are annotated in the volcano plot (see supplementary material, Figure S8). Among the up-regulated transcripts after exposure to 5 ng/ml of TGF β 1, was *Fgf18* (see supplementary material, Table S3). Levels were significantly increased

($p = 5 \times 10^{-12}$, average reads 172 versus 27) after 24 h in culture. We undertook RT-qPCR for *Fgf18*, and confirmed its significant up-regulation (see supplementary material, Figure S9). RT-qPCR showed that *Fgf18* was also expressed in native ureters harvested between E13 and birth (see supplementary material, Figure 3). Cultures exposed to exogenous TGF β 1 for 6 days showed a significant increase of *Fgf18* versus time-matched controls ($p = 0.03$, average reads 143 compared with 8). Reasoning that FGF18 might affect ureter development, E15 explants were studied: with basal media alone; with basal media supplemented with 200 ng/ml FGF18, a concentration effective in chondrocyte proliferation assays [32]; with basal media supplemented with TGF β 1; or with both exogenous FGF18 and TGF β 1. Addition of FGF18 alone produced a modest and significant elongation of the ureter tube versus controls. FGF18 did not, however, ameliorate TGF β 1 induced dysmorphogenesis (see supplementary material, Figure S10).

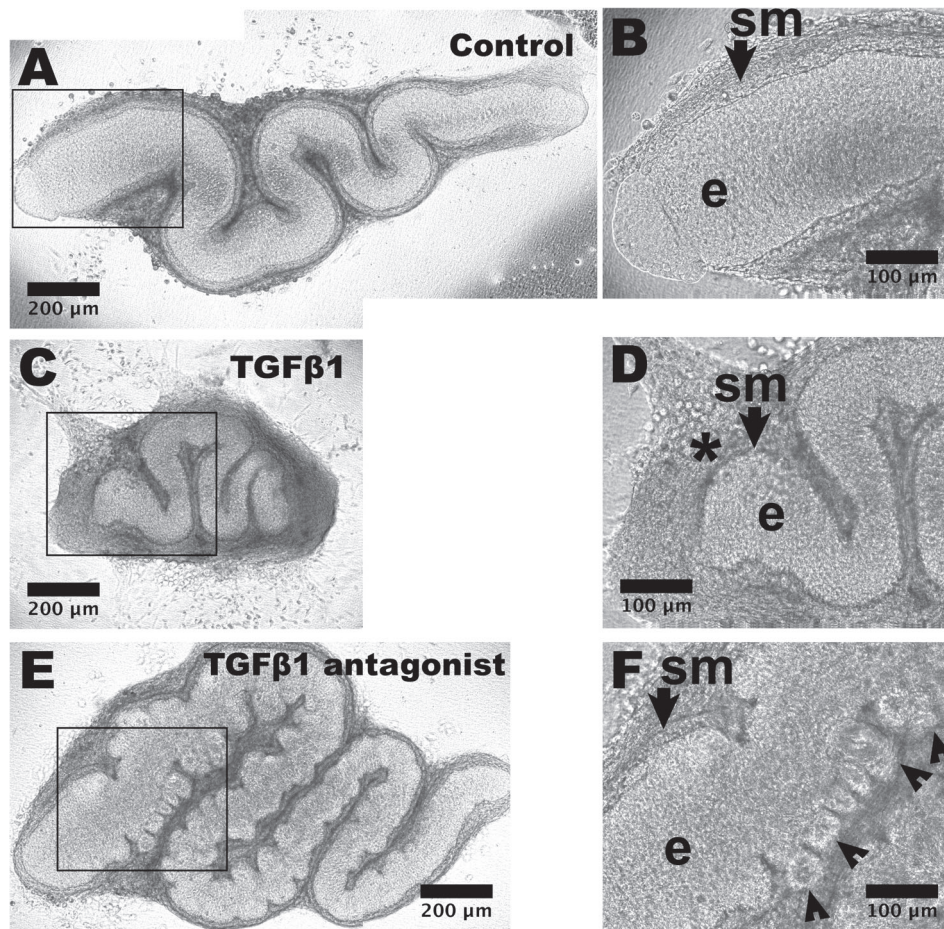


Figure 3. Gross morphology of E15 ureter explants. Explants viewed from above as whole mounts at day 6 of culture. (A) An organ fed basal media only shows a snake-like appearance, with high power of the proximal part (boxed) shown in (B). The SM layer (*sm*, arrowed) and epithelium (*e*) are indicated. (C) An organ fed with media supplemented with 5 ng/ml TGF β 1. Note that it is smaller than the control organ and it has cocooned appearance. In the high power view (D), the ureter tube is surrounded by a prominent interstitial cell layer (*asterisk*). (E) Organ after 6 days of culture fed with media supplemented with 10 μ M LY2109761 that inhibits TGF β RI/TGF β RII kinase. Note the overgrown appearance compared with the control organ, with numerous bud-like structures protruding from the epithelial tube. Some of these are visualised (arrowheads) in the high power image (F).

RNA sequencing of explants after 24 h exposure to TGF β 1 found a numerically modest but statistically significant down-regulation of *Fgf10*, which encodes FGF10, a recognised urothelial mitogen [33]. Although RT-qPCR showed only a non-significant tendency for *Fgf10* levels to fall (see supplementary material, Figure S9), we tested whether exogenous FGF10 might affect ureter growth. In these experiments (Figure 6) basal media was supplemented with 500 ng/ml FGF10, a concentration that restores ureteric bud growth in embryonic mouse kidneys with defective receptor tyrosine kinase signalling [34]. These cultures showed significantly increased lengths versus controls. In other cultures, media was supplemented with both FGF10 and TGF β 1. Here, although the cocooning effect of TGF β 1 was still evident, the TGF β 1-induced deceleration in linear growth was overcome. Immunostaining revealed FGF10 (see supplementary material, Figure S11) in human and mouse embryonic ureters *in vivo*, and in explanted mouse E15 ureters. RT-qPCR showed that *Fgf10* was expressed also in native ureters harvested between E13 and birth (see supplementary material,

Figure 3). The 24 h RNA sequence data was interrogated to seek other *Fgf* transcripts [35] and results are shown in supplementary material, Table S3. In controls, *Fgf1*, *Fgf2*, *Fgf7*, *Fgf11*, *Fgf10*, *Fgf13* and *Fgf14* were each robustly expressed (average reads >100), *Fgf5*, *Fgf9*, *Fgf12*, *Fgf18* and *Fgf20* were moderately expressed (average reads 10–100), while *Fgf3*, *Fgf4*, *Fgf6*, *Fgf8*, *Fgf15*, *Fgf16*, *Fgf21*, *Fgf22* and *Fgf23* were barely or not expressed (reads 0–9). Regarding receptors that transduce FGF signals, robust levels (reads >100) of *Fgfr1*, *Fgfr2*, *Fgfr3* and *Fgfr4* were detected in controls.

TGF β receptor blockade in ureter culture

As described above, explanted E15 ureters expressed transcripts of *Tgfb1*, *Tgfb2* and *Tgfb3*, as well as from *Tgfr1* and *Tgfr2*, the genes coding for their signal transducing receptors. This raised the possibility that endogenous TGF β ligands affect differentiation. Accordingly, we supplemented basal media with either LY2109761, that inhibits TGF β RI/TGF β RII kinase activity [36], or SB431542, that inhibits TGF β RI kinase

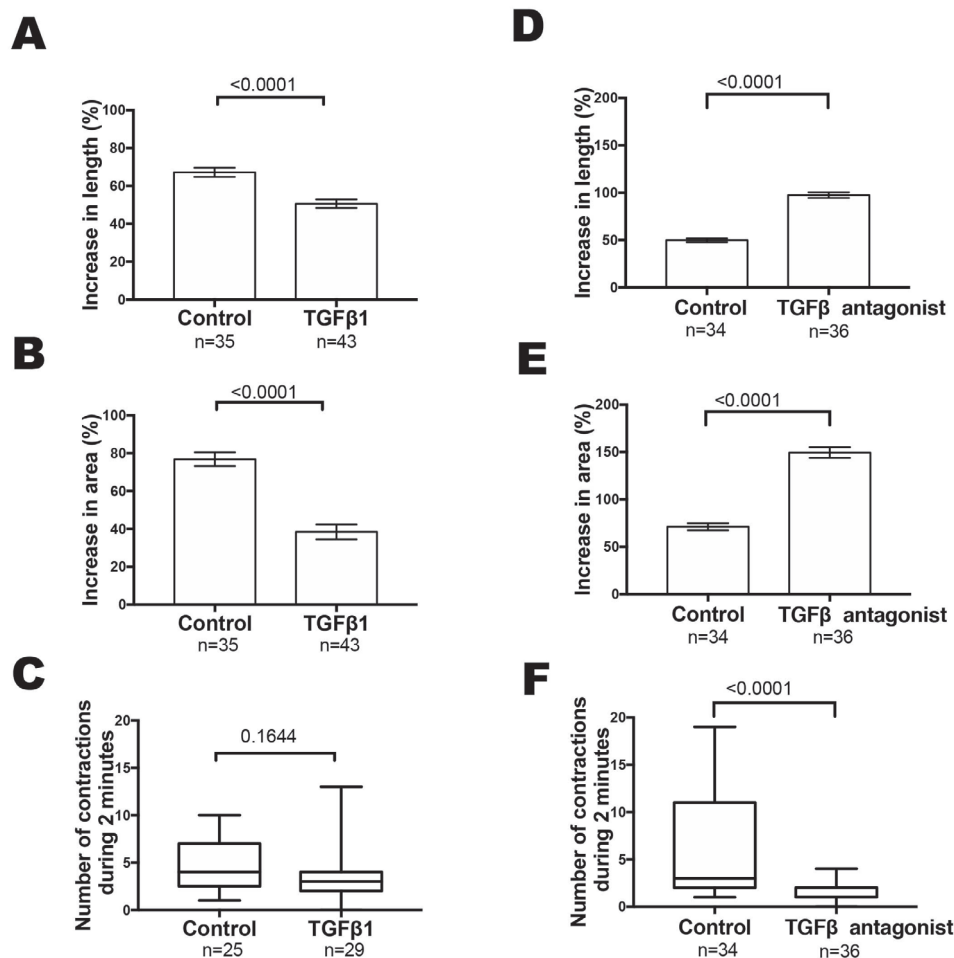


Figure 4. Quantification of growth and peristalsis in E15 ureter explants assessed at day 6 of culture. (A–C) Explants exposed to exogenous 5 ng/ml TGFβ1 showed significantly less ($p < 0.001$) elongation compared with explants fed basal media alone (A). A similar conclusion was made regarding the explant area ($p < 0.001$) (B). In both, growth of each explant was expressed as the percent increase over the length or area of the same explant measured on the day when it was explanted. Exogenous TGFβ1 did not significantly affect the number of contractions measured during 2 min (C). (D,E,F) Organs fed with basal media supplemented with 10 μM LY2109761, a molecule that inhibits TGFβRI/TGFβRII kinase. LY2109761 significantly increased ureter growth assessed as both length (D) and area compared with explants fed basal media alone. LY2109761 significantly decreased the number of ureter contractions recorded during 2 min compared with controls (F). Data are depicted as either mean ± SEM or median, interquartile range and range, as appropriate for the distribution of data points. Numbers of organs assessed are indicated on the graphs under the horizontal axes.

[37]. LY2109761 (10 μM) resulted in ureter overgrowth, with bud-like structures initiated from the urothelial tube, most prominent proximally (Figure 3E,F). Inhibition of TGFβ1 also caused enhanced linear and area growth (Figure 4D,E). In E15 ureters exposed to LY2109761, peristalsis was significantly decreased versus controls (Figure 4F). As assessed by histology of day 6 organs (Figure 5), in LY2109761 explants we visualised pocket-like protrusions from the main lumen terminating in bud-like structures containing clusters of BrdU positive cells. SM over these buds appeared attenuated (Figure 5D). As assessed by BrdU incorporation, after 24 h of culture (see supplementary material, Figure S7), in E15 organs exposed to TGFβ receptor blockade there was no change in the SM compartment, a significant ($p = 0.0086$) decrease in the adventitial compartment, and an increase approaching significance ($p = 0.0699$) in the epithelial compartment. As for E15 explants, E13 rudiments exposed to LY2109761

also acquired bud-like structures (see supplementary material, Figure S6), although growth was not formally quantified. SB431542, a different type of TGFβ receptor blocker, also resulted in bud-like structures in E15 explants, and it caused an increase in ureter tube area when applied at 10 or 20 μM (see supplementary material, Figure S12).

The cocooning effect of exogenous TGFβ1 and its growth decelerating effect on area were partly abrogated (see supplementary material, Figure S13) by LY2109761. This goes some way to prove that the dysmorphic effects of exogenous TGFβ1 were mediated through TGFβRI/TGFβRII.

Discussion

This study showed that TGFβ axis molecules are detected in both human and mouse developing ureters.

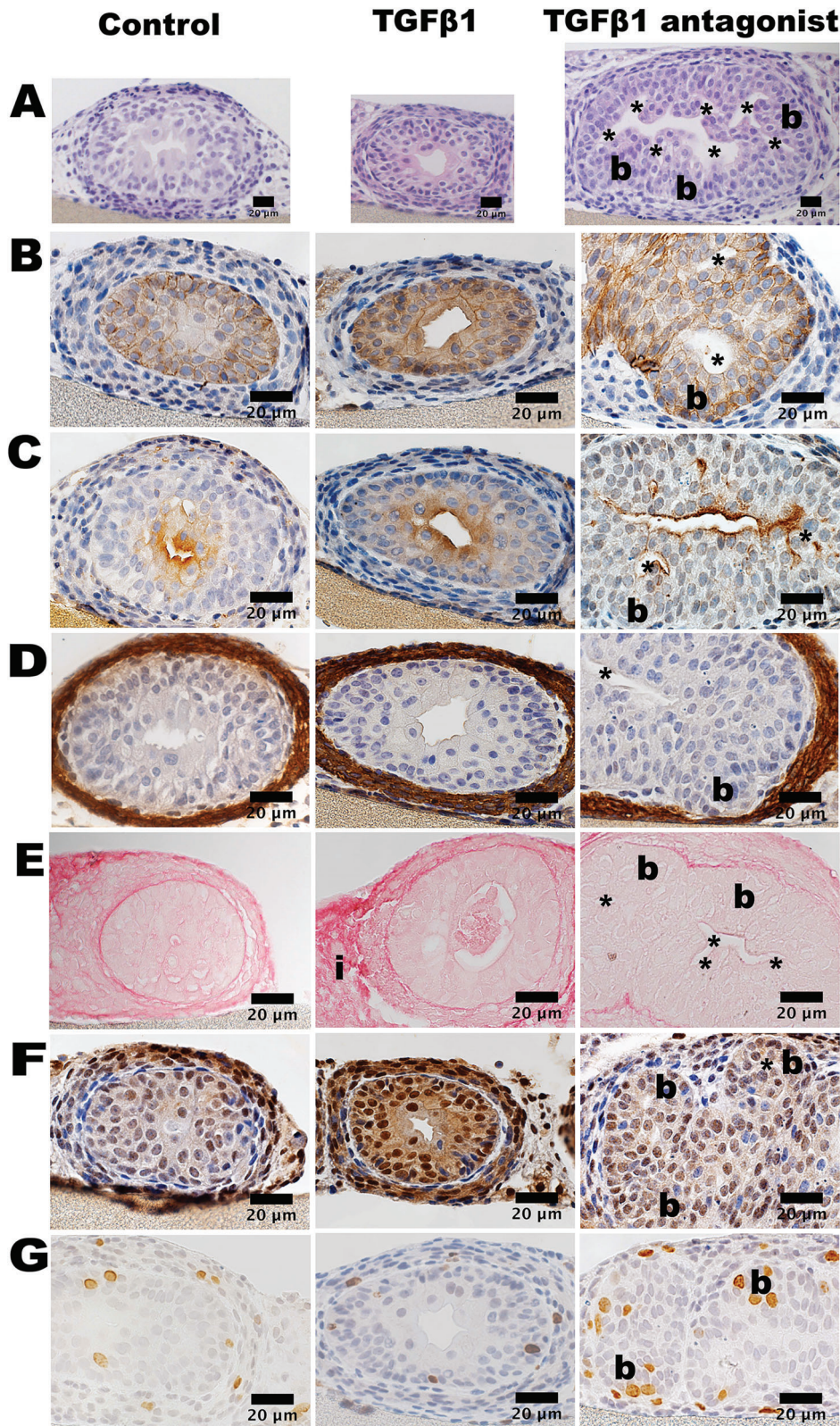


Figure 5. Histology of cultured E15 ureters. The first column depicts sections of organs fed basal media alone (Control); the second depicts transverse sections of organs exposed to exogenous 5 ng/ml TGFβ1 (*TGFβ1*); and the third depicts transverse sections of organs exposed to TGFβ blocker LY2109761 (*TGFβ1 antagonist*). Sections were counterstained with haematoxylin apart from E. (A) Eosin stained sections reveal the smaller profile of the TGFβ1 exposed ureter and the larger profile of the LY2109761 exposed ureter versus control. The lumen in the LY2109761 exposed ureter had extensions (asterisks) from the main lumen. (B) CDH1 and (C) UPKII immunostaining (brown). In the LY2109761 exposed organ note the bud-like structure (b). (D) In all three conditions, an αSMA immunostained layer (brown) was noted around the urothelium. This layer appeared attenuated over the bud in the LY2109761 exposed ureters. (E) Picrosirius red staining (red) was prominent in adventitial tissue (i) in TGFβ1 exposed organs. (F) pSMAD2 immunostaining (brown) detected positive nuclei in the three conditions. (G) BrdU immunostained (brown) nuclei were detected in both epithelial and surrounding layers in all conditions. In the organ exposed to LY2109761, clusters of positive nuclei were detected in bud-like structures. Bars, 20 μm.

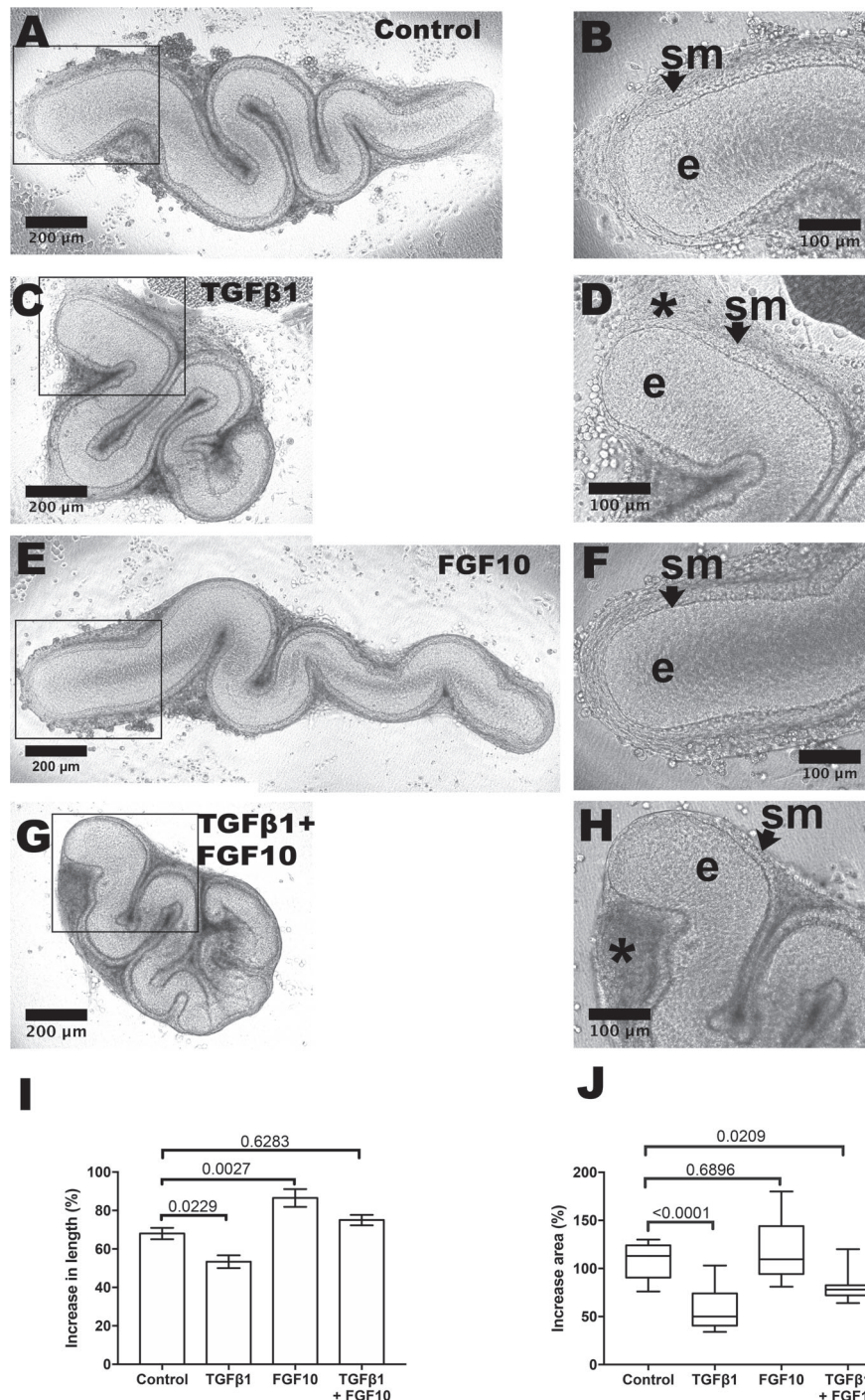


Figure 6. Effects of FGF10 in organ culture. (A–H) Explants viewed at day 6. (A) Organ fed basal media only, with high power of the boxed area shown in (B). SM (*sm*, arrowed) and epithelial (*e*) zones are indicated. (C,D) Organ fed with basal media supplemented with 5 ng/ml TGFβ1 has a cocoon-like appearance. Interstitial zone indicated by asterisk. (E,F) Organ fed with basal media supplemented with 500 ng/ml FGF10. Note the apparent increased length versus organ fed basal media alone. (G,H) Organ fed with basal media supplemented with both 5 ng/ml TGFβ1 and 500 ng/ml FGF10. Cocooning is still apparent with prominent interstitial tissue (*) but the length of the tube appears increased versus the organ exposed to TGFβ1 alone. (I,J) Quantification of increases in urothelial tube length (I) and area (J) show that FGF10 ($n = 12$) caused significant linear growth versus basal media alone ($n = 13$). Addition of TGFβ1 ($n = 13$) caused significant reduction in linear and area growth versus basal media alone. When FGF10 was added together with TGFβ1 ($n = 13$) the negative effect of the latter on linear growth was overcome.

Moreover, unique dysmorphic phenotypes were generated by adding exogenous TGFβ1 (i.e. inhibition of growth and generation of a cocoon-like phenotype) or by adding TGFβ receptor blockers (i.e. acceleration of linear growth accompanied by formation of epithelial ‘buds’).

Previous studies defined molecules directing ureteric bud initiation, branching of its top end, and the connection of its distal end to the bladder. These included secreted molecules such as glial cell line-derived growth factor (GDNF), bone morphogenetic proteins (BMPs), FGFs and retinoic acid [8,34,38,39]. Growth factor

control of stalk development has been studied less. The embryonic urothelium secretes sonic hedgehog (SHH) that induces BMP4 in nearby mesenchyme: here BMP4 leads to induction of SM proteins [40,41]. SHH signalling is also required for pacemaker maturation [42], while Cajal-like cells in the SM layer of the ureteric express KIT, a growth factor receptor needed for their function [5]. Before our study, however, little had been reported about the possible roles for TGF β in the embryonic ureter.

We discovered that blocking endogenous TGF β , with either of two receptor inhibitors, generated epithelial overgrowth in embryonic ureters, thus revealing a previously unreported regulatory role for the TGF β axis in morphogenesis of the ureteric stalk. The phenotype may in part be explained by the fact that, based on experiments with cultures of postnatal urothelia, exogenous TGF β 1 inhibits proliferation [43]. Thus, in the current context, blockade would be associated with overgrowth, as manifested by aberrant bud-like structures. The current results observed after blockade of endogenous TGF β are broadly consistent with the observation that a monoclonal antibody to TGF β 1 administered to pregnant rabbits increased the incidence of ureter malformations in offspring [44]. The dysmorphic effects of TGF β blockade on developing ureters have parallels in other organs. Antibody mediated TGF β 1 blockade causes accelerated nephron tubule formation in metanephric kidney organ culture [15], and inhibiting TGF β RI in embryonic lungs increases branching [45]. In contrast to the bud-like structures observed in the ureter stalk, this lung phenotype appears confined to the distal sections of the bronchial tube, where branching normally occurs [45]. The bud-like phenotype of the ureter upon TGF β R blockade appear morphologically similar to that reported in embryonic ureter stalks exposed to GDNF or FGF7 [46]. We speculate that these buds, to a small extent, mimic the phenotype of inverted papillomas, a rare human ureter disorder. In this disease, the ureteric urothelium extends cords of epithelial cells in away from the organ's lumen [47,48]. In future, it may be informative to analyse expression of TGF β axis molecules in these benign tumours.

This study additionally discovered that exogenous TGF β 1 causes embryonic ureter malformations, generating a phenotype distinct from that caused by TGF β blockade. This supports the idea that an overactive TGF β axis contributes to dysmorphogenesis in human renal tract malformations [17–19]. Exogenous TGF β 1 caused the explanted ureteric tube to become encased in a cocoon-like structure. This may have generated a physical constraint limiting ureter tube growth, and indeed we did not find a decreased proliferative index in explants. On the other hand, exogenous TGF β 1 is reported to decrease proliferation of postnatal urothelia [43] and ureteric bud tips [49], and it compromises branching morphogenesis in salivary glands [31,50] and lung [45]. Another study reported that embryonic rat ureters exposed to TGF β had impaired urothelial and

SM proliferation [51]. That study [51], however, neither showed images of growing organs nor assessed gene expression.

In future, it will be important to pinpoint the intracellular signalling mechanisms of TGF β and in ureter development. This is a potentially complex field, with numerous pathways potentially involved [14]. The canonical, TGF β signalling pathway involves SMAD2 and SMAD3 that form complexes with SMAD4 which then move to the nucleus. Although we detected pSMAD2 on histology sections, this study did not quantify the signals. Moreover, another SMAD, SMAD7, inhibits the TGF β pathway [14]. Furthermore non-canonical TGF β signalling may be operative, too, involving p38 MAPK, JNK or NF- κ B [14]. One way forward here would be to generate a series of mutant mice, each with a deletion of specific TGF β receptors or SMADs or other intracellular signalling molecules in either the urothelium or the mesenchyme/SM or the adventitia. In this respect, it is notable that Mamo *et al* [41] used a *Tbx18Cre* driver to delete SMAD4 in differentiating SM of the ureter, noting only a modest delay in SM differentiation. In fact, TGF β signalling is also thought to enhance SM differentiation in the developing intestine [30]. The study of Mamo *et al* [41] would not have been informative with regard to potential TGF β direct effects on the differentiating urothelium and this may explain why ectopic buds, prominent after TGF β receptor inhibition in the current work, were not observed.

After 24 h of TGF β 1 exposure, the most up-regulated transcripts in the RNA sequencing sets were those encoding: platelet-derived growth factor-like (*Pdgfrl*), implicated in chondrocyte differentiation [52]; scleraxis (*Scx*), implicated in extracellular matrix molecule expression in tendons and heart [53]; chondroadherin (*Chad*), which is enriched in cartilage [54]; biglycan (*Bgn*), a matrix molecule that, like chondroadherin, is up-regulated during TGF β induced differentiation of mesenchymal stem cells towards cartilage [55]; fibronectin-1 (*Fnl1*), a matrix protein implicated in myofibroblast formation [56]; and matrix Gla protein (*Mgp*) that modulates urinary stone formation [57]. These changes were consistent with increased adventitial prominence after TGF β 1 exposure, suggesting that its composition begins to shift towards a metaplastic cartilage-like phenotype.

Fgf18 was also up-regulated in TGF β 1 exposed ureters. Rudiments also expressed *Fgfr3*, encoding the cell surface receptor for FGF18 [58]. Ours is the first report drawing attention to whether this ligand is expressed in the embryonic ureter, and exploring its potential relation to morphogenesis. When recombinant FGF18 was added to ureteric explants fed basal media alone, a small increase in linear growth occurred but exogenous FGF18 did not impact on TGF β 1-induced dysmorphogenesis. Further experiments are needed to determine whether endogenous *Fgf18* affects ureter development. FGF18 is related to FGF8 and FGF17 [58] but *Fgf8* and *Fgf17* transcripts were barely detectable in

ureter rudiments. *FGF18* polymorphisms are associated with facial clefting, *FGFR3* mutations cause skeletal dysplasias [35], and *Fgf18* deleted mice have delayed chondrocyte differentiation [59]. Mice lacking FGF18 have impaired alveolar epithelial growth in development [60], and *Fgfr3* mutant mice have enhanced intestinal crypt proliferation [61]. Other studies link FGF18 and TGF β biology. In hair, TGF β 2 and FGF18 respectively accelerate and delay telogen-to-anagen transition in which new hair shafts are generated from stem cells [62]. Finally, in bone cultures, TGF β 1 up-regulates *Fgf18*, with increased FGFRIII phosphorylation [32].

Among down-regulated transcripts were those encoding: sushi, nidogen and EGF-like domains 1 (*Sned1*), an extracellular matrix protein found in embryonic kidneys [63] and implicated in tumour invasion [64]; hippocalcin (*Hpca*), a calcium sensor implicated in neurodegeneration [65]; solute carrier family 26A7 (*Slc26a7*), a Cl⁻/HCO₃⁻ exchanger [66]; solute carrier family 26A1 (*Slc4a1*), an anion exchanger [67]; and tenascin XB (*Tnxb*). *TNXB* mutations cause human urinary tract malformations and healthy urothelia express tenascin XB [68], a protein that regulates TGF β 1 bioavailability [69]. Robust levels of the following transcripts were detected at days 1 and 6 of culture in controls: *Shh*, *Ptch1*, *Smo*, *Gli1*, *Gli2* and *Bmp4*, encoding hedgehog pathway molecules that generate SM [70]; and *Rara*, *Rarb*, *Rarg*, *Sox9*, *Tbx18* and *Tshz3*, encoding urinary tract transcription factors [3,70–73]. Exogenous TGF β 1 did not alter these transcripts after correction for multiple comparisons. FGF10 is mitogenic for urothelia [33] and stimulates amniotic stem cells to acquire urothelial characteristics [74]. We noted a tendency for down-regulated *Fgf10* upon exposure to TGF β 1. When FGF10 was added to cultures, the growth inhibiting effect of TGF β 1 was abrogated. This introduces the idea that the dysmorphic effects of TGF β 1 can be modified by other growth factors expressed in the embryonic ureter. Notably, in an *ex vivo* model, exogenous TGF β 1 inhibited *Fgf10* expression in prostate-related mesenchyme, an effect mediated through the *Fgf10* promoter [75].

Collectively, these observations reveal an unsuspected regulatory role for endogenous TGF β signalling in embryonic ureters, fine-tuning morphogenesis. The results also support the hypothesis that up-regulation of TGF β axis molecules plays roles in the pathobiology of ureter malformations. Further experiments are needed to unravel the intracellular signalling mechanisms involved in these dysmorphic responses.

Acknowledgements

We acknowledge grant support from: the Medical Research Council MR/L002744/1 and MR/K026739/1 (ASW); Horizon 2020 Marie Skłodowska-Curie Actions Initial Training Network RENALTRACT (942937) (ASW, NJG, FL); Newlife Foundation (ASW); Kidney Research UK Non-Clinical Training Fellowship (NAR).

Histology Core Facility equipment was purchased with grants from the University of Manchester Strategic Fund. Human embryonic material was provided by the Joint MRC and Wellcome Trust (MR/R006237/1) Human Developmental Biology Resource (www.hdbr.org). We thank Laurent Fasano, Xavier Caubit and Irene Sanchez Martin (Aix-Marseille Université, France) for technical advice regarding measurement of embryonic mouse ureter peristalsis. We thank Andreas Kispert, Anna-Carina Weiss and Jaskiran Kaur (Hannover Medical School, Germany) for technical advice regarding histology of embryonic mouse ureters.

Author contributions statement

ASW, FML and NAG conceived and designed the study. FML, NAR and LAHZ undertook analyses. All authors contributed to data interpretation. ASW and FML drafted the paper. All authors approved the final version of the paper.

References

1. Wu XR, Kong XP, Pellicer A, et al. Uroplakins in urothelial biology, function, and disease. *Kidney Int* 2009; **75**: 1153–1165.
2. Bohnenpoll T, Feraric S, Nattkemper M, et al. Diversification of cell lineages in ureter development. *J Am Soc Nephrol* 2017; **28**: 1792–1801.
3. Caubit X, Lye CM, Martin E, et al. Teashirt 3 is necessary for ureteral smooth muscle differentiation downstream of SHH and BMP4. *Development* 2008; **135**: 3301–3310.
4. Hurtado R, Bub G, Herzlinger D. A molecular signature of tissues with pacemaker activity in the heart and upper urinary tract involves coexpressed hyperpolarization-activated cation and T-type Ca²⁺ channels. *FASEB J* 2014; **28**: 730–739.
5. David SG, Cebrian C, Vaughan ED Jr, et al. c-kit and ureteral peristalsis. *J Urol* 2005; **173**: 292–295.
6. Woolf AS, Davies JA. Cell biology of ureter development. *J Am Soc Nephrol* 2013; **24**: 19–15.
7. Lye CM, Fasano L, Woolf AS. Ureter myogenesis: putting *Teashirt* into context. *J Am Soc Nephrol* 2010; **21**: 24–30.
8. Chia I, Grote D, Marcotte M, et al. Nephric duct insertion is a crucial step in urinary tract maturation that is regulated by a Gata3-Raldh2-Ret molecular network in mice. *Development* 2011; **138**: 2089–2097.
9. Woolf AS, Jenkins D. Development of the kidney. In *Heptinstall's Pathology of the Kidney* (7th edn), Jennette JC, Olson JL, Silva FG, et al. (eds). Wolters Kluwer: Philadelphia, PA, 2015; 67–89.
10. Kerecuk L, Schreuder MF, Woolf AS. Human renal tract malformations: perspectives for nephrologists. *Nat Clin Pract Nephrol* 2008; **4**: 312–325.
11. Ek S, Lidfeldt KJ, Varricio L. Fetal hydronephrosis; prevalence, natural history and postnatal consequences in an unselected population. *Acta Obstet Gynecol Scand* 2007; **86**: 1463–1466.
12. Woolf AS, Price K, Scambler PJ, et al. Evolving concepts in human renal dysplasia. *J Am Soc Nephrol* 2004; **15**: 998–1007.
13. Yang SP, Woolf AS, Yuan HT, et al. Potential biological role of transforming growth factor β 1 in human congenital kidney malformations. *Am J Pathol* 2000; **157**: 1633–1647.
14. Akhurst RJ, Hata A. Targeting the TGF β signalling pathway in disease. *Nat Rev Drug Discov* 2012; **11**: 790–811.

15. Rogers SA, Ryan G, Purchio AF, *et al.* Metanephric transforming growth factor-beta 1 regulates nephrogenesis in vitro. *Am J Physiol* 1993; **264**: F996–F1002.
16. Yang SP, Woolf AS, Quinn F, *et al.* Deregulation of renal transforming growth factor- β 1 after experimental short-term ureteric obstruction in fetal sheep. *Am J Pathol* 2001; **159**: 109–117.
17. Yang Y, Zhou X, Gao H, *et al.* The expression of epidermal growth factor and transforming growth factor-beta1 in the stenotic tissue of congenital pelvi-ureteric junction obstruction in children. *J Pediatr Surg* 2003; **38**: 1656–1660.
18. Jabbar ME, Goldfischer ER, Anderson AE, *et al.* Failed endopyelotomy: low expression of TGF beta regardless of the presence or absence of crossing vessels. *J Endourol* 1999; **13**: 295–298.
19. Nicotina PA, Romeo C, Arena F, *et al.* Segmental up-regulation of transforming growth factor-beta in the pathogenesis of primary megaureter. An immunocytochemical study. *Br J Urol* 1997; **80**: 946–949.
20. Chuang YH, Chuang WL, Chen SS, *et al.* Expression of transforming growth factor-beta 1 and its receptors related to the ureteric fibrosis in a rat model of obstructive uropathy. *J Urol* 2000; **163**: 1298–1303.
21. Lopes FM, Woolf AS. Serum-free organ culture of the embryonic mouse ureter. *Methods Mol Biol* 2019; **1926**: 31–38.
22. Namvar S, Woolf AS, Zeef LA, *et al.* Functional molecules in mesothelial-to-mesenchymal transition revealed by transcriptome analyses. *J Pathol* 2018; **245**: 491–501.
23. Bolger AM, Lohse M, Usadel B. Trimmomatic: a flexible trimmer for Illumina sequence data. *Bioinformatics* 2014; **30**: 2114–2120.
24. Dobin A, Davis CA, Schlesinger F, *et al.* STAR: ultrafast universal RNA-seq aligner. *Bioinformatics* 2013; **29**: 15–21.
25. Love MI, Huber W, Anders S. Moderated estimation of fold change and dispersion for RNA-seq data with DESeq2. *Genome Biol* 2014; **15**: 550.
26. Waldrop FS, Puchtler H. Light microscopic distinction of collagens in hepatic cirrhosis. *Histochemistry* 1982; **74**: 487–491.
27. Smeulders N, Woolf AS, Wilcox DT. Smooth muscle differentiation and cell turnover in mouse detrusor development. *J Urol* 2002; **167**: 385–390.
28. Jenkins LM, Horst B, Lancaster CL, *et al.* Dually modified transmembrane proteoglycans in development and disease. *Cytokine Growth Factor Rev* 2018; **39**: 124–136.
29. Clark AT, Young RJ, Bertram JF. *In vitro* studies on the roles of transforming growth factor- β 1 in rat metanephric development. *Kidney Int* 2001; **59**: 1641–1653.
30. Coletta R, Roberts NA, Randles MJ, *et al.* Exogenous transforming growth factor- β 1 enhances smooth muscle differentiation in embryonic mouse jejunal explants. *J Tissue Eng Regen Med* 2018; **12**: 252–264.
31. Hardman P, Landels E, Woolf AS, *et al.* Transforming growth factor- β 1 inhibits growth and branching morphogenesis in embryonic mouse submandibular and sublingual glands *in vitro*. *Dev Growth Differ* 1994; **36**: 567–577.
32. Mukherjee A, Dong SS, Clemens T, *et al.* Co-ordination of TGF-beta and FGF signaling pathways in bone organ cultures. *Mech Dev* 2005; **122**: 557–571.
33. Bagai S, Rubio E, Cheng JF, *et al.* Fibroblast growth factor-10 is a mitogen for urothelial cells. *J Biol Chem* 2001; **277**: 23828–23837.
34. Pitera JE, Woolf AS, Basson AM, *et al.* *Sprouty1* haploinsufficiency prevents renal agenesis in a model of Fraser syndrome. *J Am Soc Nephrol* 2012; **23**: 1790–1796.
35. Ornitz DM, Itoh N. The fibroblast growth factor signaling pathway. *Wiley Interdiscip Rev Dev Biol* 2015; **4**: 215–266.
36. Melisi D, Ishiyama S, Sclabas GM, *et al.* LY2109761, a novel transforming growth factor beta receptor type I and type II dual inhibitor, as a therapeutic approach to suppressing pancreatic cancer metastasis. *Mol Cancer Ther* 2008; **7**: 829–840.
37. Laping NJ, Grygielko E, Mathur A, *et al.* Inhibition of transforming growth factor (TGF)-beta 1-induced extracellular matrix with a novel inhibitor of the TGF-beta type I receptor kinase activity: SB-431542. *Mol Pharmacol* 2002; **62**: 58–64.
38. Pitera JE, Scambler PJ, Woolf AS. Fras1, a basement membrane-associated protein mutated in Fraser syndrome, mediates both the initiation of the mammalian kidney and the integrity of renal glomeruli. *Hum Mol Genet* 2008; **17**: 3953–3964.
39. Sims-Lucas S, Cusack B, Eswarakumar VP, *et al.* Independent roles of Fgfr2 and Frs2alpha in ureteric epithelium. *Development* 2011; **138**: 1275–1280.
40. Yu J, Carroll TJ, McMahon AP. Sonic hedgehog regulates proliferation and differentiation of mesenchymal cells in the mouse metanephric kidney. *Development* 2002; **129**: 5301–5312.
41. Mamo TM, Wittern AB, Kleppa MJ, *et al.* BMP4 uses several different effector pathways to regulate proliferation and differentiation in the epithelial and mesenchymal tissue compartments of the developing mouse ureter. *Hum Mol Genet* 2017; **26**: 3553–3563.
42. Cain JE, Islam E, Haxho F, *et al.* GLI3 repressor controls functional development of the mouse ureter. *J Clin Invest* 2011; **121**: 1199–1206.
43. de Boer WI, Vermeij M, Diez de Medina SG, *et al.* Functions of fibroblast and transforming growth factors in primary organoid-like cultures of normal human urothelium. *Lab Invest* 1996; **75**: 147–156.
44. Hilbisch KG, Martin JA, Stauber AJ, *et al.* TGF- β 1 monoclonal antibody: assessment of embryo-fetal toxicity in rats and rabbits. *Birth Defects Res B Dev Reprod Toxicol* 2016; **107**: 174–184.
45. Gleghorn JP, Kwak J, Pavlovich AL, *et al.* Inhibitory morphogens and monopodial branching of the embryonic chicken lung. *Dev Dyn* 2012; **241**: 852–862.
46. Bush KT, Vaughn DA, Li X, *et al.* Development and differentiation of the ureteric bud into the ureter in the absence of a kidney collecting system. *Dev Biol* 2006; **298**: 571–584.
47. Luo JD, Wang P, Chen J, *et al.* Upper urinary tract inverted papillomas: report of 10 cases. *Oncol Lett* 2012; **4**: 71–74.
48. Kilciler M, Bedir S, Erdemir F, *et al.* Evaluation of urinary inverted papillomas: a report of 13 cases and literature review. *Kaohsiung J Med Sci* 2008; **24**: 25–30.
49. Bush KT, Sakurai H, Steer DL, *et al.* TGF-beta superfamily members modulate growth, branching, shaping, and patterning of the ureteric bud. *Dev Biol* 2004; **266**: 285–298.
50. Janebodin K, Buranaphatthana W, Ieronimakis N, *et al.* An *in vitro* culture system for long-term expansion of epithelial and mesenchymal salivary gland cells: role of TGF- β 1 in salivary gland epithelial and mesenchymal differentiation. *Biomed Res Int* 2013; **2013**: 815895.
51. Ozturk E, Telli O, Gokce MI, *et al.* Effects of transforming growth factor on the developing embryonic ureter: an *in-vitro* megaureter model in mice. *J Pediatr Urol* 2016; **12**: 310.e1–310.e4.
52. Kawata K, Kubota S, Eguchi T, *et al.* A tumor suppressor gene product, platelet-derived growth factor receptor-like protein controls chondrocyte proliferation and differentiation. *J Cell Biochem* 2017; **118**: 4033–4044.
53. Czubryt MP. A tale of 2 tissues: the overlapping role of scleraxis in tendons and the heart. *Can J Physiol Pharmacol* 2014; **92**: 707–712.
54. Haglund L, Ouellet J, Roughley P. Variation in chondroadherin abundance and fragmentation in the human scoliotic disc. *Spine* 2009; **34**: 1513–1515.
55. Barry F, Boynton RE, Liu B, *et al.* Chondrogenic differentiation of mesenchymal stem cells from bone marrow: differentiation-dependent gene expression of matrix components. *Exp Cell Res* 2001; **268**: 189–200.
56. Gabbiani G. The myofibroblast in wound healing and fibrocontractive diseases. *J Pathol* 2003; **200**: 500–503.

57. Lu X, Gao B, Yasui T, *et al.* Matrix Gla protein is involved in crystal formation in kidney of hyperoxaluric rats. *Kidney Blood Press Res* 2013; **37**: 15–23.
58. Jovelin R, Yan YL, He X, *et al.* Evolution of developmental regulation in the vertebrate FgfD subfamily. *J Exp Zool B Mol Dev Evol* 2010; **314**: 33–56.
59. Liu Z, Lavine KJ, Hung IH, *et al.* FGF18 is required for early chondrocyte proliferation, hypertrophy and vascular invasion of the growth plate. *Dev Biol* 2007; **302**: 80–91.
60. Usui H, Shibayama M, Ohbayashi N, *et al.* Fgf18 is required for embryonic lung alveolar development. *Biochem Biophys Res Commun* 2004; **322**: 887–892.
61. Arnaud-Dabernat S, Yadav D, Sarvetnick N. FGFR3 contributes to intestinal crypt cell growth arrest. *J Cell Physiol* 2008; **216**: 261–268.
62. Plikus MV. New activators and inhibitors in the hair cycle clock: targeting stem cells' state of competence. *J Invest Dermatol* 2012; **132**: 1321–1324.
63. Leimeister C, Schumacher N, Diez H, *et al.* Cloning and expression analysis of the mouse stroma marker Snep encoding a novel nidogen domain protein. *Dev Dyn* 2004; **230**: 371–377.
64. Naba A, Clauser KR, Lamar JM, *et al.* Extracellular matrix signatures of human mammary carcinoma identify novel metastasis promoters. *Elife* 2014; **3**: e01308.
65. Rudinskiy N, Kaneko YA, Beesen AA, *et al.* Diminished hippocampin expression in Huntington's disease brain does not account for increased striatal neuron vulnerability as assessed in primary neurons. *J Neurochem* 2009; **111**: 460–472.
66. Soleimani M. SLC26 Cl-/HCO3- exchangers in the kidney: roles in health and disease. *Kidney Int* 2013; **84**: 657–666.
67. Besouw MTP, Bienias M, Walsh P, *et al.* Clinical and molecular aspects of distal renal tubular acidosis in children. *Pediatr Nephrol* 2017; **32**: 987–996.
68. Gbadegesin RA, Brophy PD, Adeyemo A, *et al.* TNXB mutations can cause vesicoureteral reflux. *J Am Soc Nephrol* 2013; **24**: 1313–1322.
69. Valcourt U, Alcaraz LB, Exposito JY, *et al.* Tenascin-X: beyond the architectural function. *Cell Adh Migr* 2015; **29**: 154–165.
70. Sheybani-Deloui S, Chi L, Staite MV, *et al.* Activated hedgehog-GLI signaling causes congenital ureteropelvic junction obstruction. *J Am Soc Nephrol* 2018; **29**: 532–544.
71. Vivante A, Kleppa MJ, Schulz J, *et al.* Mutations in TBX18 cause dominant urinary tract malformations via transcriptional dysregulation of ureter development. *Am J Hum Genet* 2015; **97**: 291–301.
72. Martin E, Caubit X, Airik R, *et al.* TSHZ3 and SOX9 regulate the timing of smooth muscle cell differentiation in the ureter by reducing myocardin activity. *PLoS One* 2013; **8**: e63721.
73. Bohnenpoll T, Weiss AC, Labuhn M, *et al.* Retinoic acid signaling maintains epithelial and mesenchymal progenitors in the developing mouse ureter. *Sci Rep* 2017; **7**: 14803.
74. Chung SS, Koh CJ. Bladder cancer cell in co-culture induces human stem cell differentiation to urothelial cells through paracrine FGF10 signaling. *In Vitro Cell Dev Biol Anim* 2013; **49**: 746–751.
75. Tomlinson DC, Grindley JC, Thomson AA. Regulation of Fgf10 gene expression in the prostate: identification of transforming growth factor-beta1 and promoter elements. *Endocrinology* 2004; **145**: 1988–1995.

SUPPLEMENTARY MATERIAL ONLINE

Supplementary materials and methods

Figure S1. Immunodetection of TGFβRI and TGFβRII in a 10-week human ureter

Figure S2. Immunodetection of TGFβRI and TGFβRII in the embryonic day 15 mouse ureter

Figure S3. RT-qPCR of mouse ureters harvested between E13 and the day of birth

Figure S4. *In situ* hybridisation of embryonic day 15 mouse ureter

Figure S5. Gross morphology and growth of explanted E15 ureters

Figure S6. E13 ureter explants viewed as whole mounts in culture

Figure S7. Quantification of BrdU uptake 24 h after explanting embryonic day 15 ureters into culture

Figure S8. RNA-sequencing data displayed as a volcano plot, comparing TGFβ1 exposed and control cultures at 24 h after being explanted

Figure S9. RT-qPCR analyses of ureter explants

Figure S10. Effects of addition of FGF18 to mouse E15 ureters in organ culture

Figure S11. Immunostaining for FGF10

Figure S12. Effects of SB431542, a TGFβRI kinase inhibitor, on E15 ureter organ cultures

Figure S13. Effects of adding both TGFβ1 and a TGFβ receptor blocker

Table S1. Transcripts encoding TGFβ family members and their receptors in explanted embryonic ureters

Table S2. The most significantly changed transcripts in TGFβ1 exposed ureters versus control ureters on day 1 of E15 organ culture

Table S3. Transcripts encoding FGF family members and their receptors, as detected and quantified in the RNA-sequencing analyses